Acta Cryst. (1986). B42, 26–32

Charge Density Distribution in Thiosulfates: $Na_2S_2O_3$ and $MgS_2O_3.6H_2O$

BY J. W. BATS AND H. FUESS

Institut für Kristallographie und Mineralogie der Universität Frankfurt, Senckenberganlage 30, *D*-6000 *Frankfurt/Main* 1, *Federal Republic of Germany*

(*Received* 8 *December* 1984; *accepted* 8 *July* 1985)

Abstract

Static deformation densities in both $Na_2S_2O_3$ and $MgS_2O_3.6H_2O$ were derived by multipole refinement of X-ray diffraction data collected at 120 K. The deformation density is very similar in both thiosulfate groups. The lone-pair density at the hydrate O atoms is affected by cation and hydrogen-bond influences. Net atomic charges obtained by fuzzy-boundary integration are unrealistic for Na and Mg owing to the diffuse nature of the metal 3*s* shell. For H atoms contracted valence shells ($\kappa_H = 1{\cdot}4$) should be used. Dipole moments for the hydrate molecules range from 1·6 to 2·4 D (1 D = $3{\cdot}3 \times 10^{-30}$ Cm) depending on the partitioning model employed.

Introduction

The present work describes a charge density study of thiosulfates. The deformation density in $MgS_2O_3.6H_2O$ has been determined by *X*-*N* methods by Elerman, Bats & Fuess (1983). Those data are further analyzed in the present study. In addition, low-temperature X-ray and neutron diffraction data have been reported for $Na_2S_2O_3$ (Teng, Fuess & Bats, 1984). Using those data the electron density distribution of that compound is studied. Results on both thiosulfates are compared.

The first part of this paper deals with deformation refinements of both compounds, followed by a description of the electron density distribution. In the second part, the observed electron density is analyzed by spatial partitioning over atomic densities. In the final part the dipole moments for the hydrate molecules are derived.

Deformation refinement*

Deformation refinements were performed on the X-ray diffraction data sets of $Na_2S_2O_3$ and $MgS_2O_3.6H_2O$. Calculations were with the multipole expansion program *MOLLY* (Hansen & Coppens, 1978). For S and O, multipoles up to the hexadecapole level ($l = 4$) were included, although many of them could be fixed by imposing a molecular symmetry higher than the crystallographic symmetry. For the H atoms of the hydrates, only a monopole and one dipole function along the H–O bond axis were used; the Na and Mg cations were constrained to spherical symmetry by the use of a monopole deformation function only. Monopoles were represented by spherical atomic valence shells (Fukamachi, 1971). A radial expansion coefficient κ is refined together with the monopole population parameter. The multipole functions with $l > 0$ all had a radial function $r^{n_l} \exp(-\zeta r)$ with only one ζ value per atom; the n_l and final ζ values are reported in Table 1. An isotropic extinction coefficient (type 1, Lorentzian distribution) was refined as described by Becker & Coppens (1974). The local coordinate systems used are represented in Fig. 1.

$Na_2S_2O_3$

A preliminary *X*-*X* density of $Na_2S_2O_3$ (Teng, Fuess & Bats, 1981) appeared rather noisy. Therefore, it seemed useful to constrain chemically equivalent

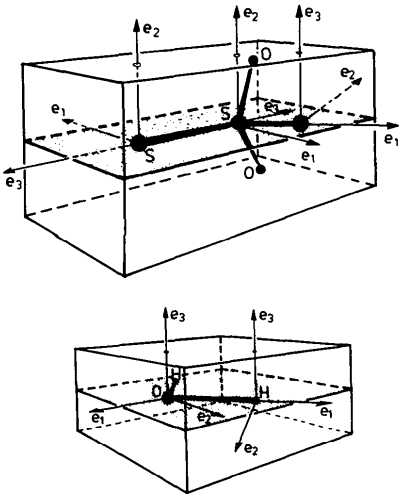

Fig. 1. Local orthonormal coordinate systems used in the multipole refinement.

* Tables of multipole coefficients and radial parameters have been deposited with the British Library Lending Division as Supplementary Publication No. SUP 42405 (5 pp.). Copies may be obtained through The Executive Secretary, International Union of Crystallography, 5 Abbey Square, Chester CH1 2HU, England.

0108-7681/86/010026-07$01.50

© 1986 International Union of Crystallography

Table 1. *Parameters of the radial parts of the multipole functions:* $r^{n_l} \exp(-\zeta r)$ *and* κ *values of the monopoles*

Radial parameters in $Na_2S_2O_3$

		n_l		
l	Na	S(1)	S(2)	O
1	—	4	4	2
2	—	4	4	2
3	—	6	6	3
4	—	8	8	4
ζ	—	2·59 (16)	4·43 (8)	4·71 (30)
κ	1·6 (3)	0·994 (4)	0·965 (7)	0·988 (2)

Radial parameters in $MgS_2O_3.6H_2O$

		n_l				
l	Mg	S(1)	S(2)	O(1)	O(3)	H
1	—	4	4	2	2	2
2	—	4	4	2	2	—
3	—	6	6	3	3	—
4	—	8	8	4	4	—
ζ	—	3.20 (30)	4.63 (14)	7.2 (8)	3.47 (16)	5.4 (5)
κ	1·02 (6)	0·970 (6)	0·931 (8)	0·981 (2)	0·971 (3)	1·16 (3)

but crystallographically independent groups to have identical deformation parameters. Thus both S atoms were constrained to $3m$ symmetry, identical monopoles were assigned to both Na atoms, and the three O atoms were given identical deformation parameters with imposed symmetry m. Two refinement models were used. In model *A* the deformation parameters including κ values were refined together with the positional and thermal parameters, and scale and extinction factors. In model *B* the O positional parameters were fixed to the values of the neutron diffraction study, while all other parameters were refined as for model *A*. After initial convergence was reached, further refinement was carried out including the exponents ζ of the deformation functions. The refinement converged at $wR = 0{\cdot}023$ for both models. For comparison the conventional structure refinement gave $wR = 0{\cdot}029$. Larger improvements in R values have been observed for multipole refinements of organic crystals. The relatively minor improvement in the present case can be attributed to the unfavorable valence-to-core ratio. At this stage an inspection of residual structure factors revealed a considerable number of relatively weak reflections with $F_{obs} \gg F_{calc}$, which were attributed to multiple reflections. 180 reflections had $F_{obs}/F_{calc} > 2$ and were deleted from the data set. Refinement on the remaining 3456 reflections converged at $R = 0{\cdot}026$, $wR = 0{\cdot}021$, $S = 1{\cdot}26$; extinction coefficient $g = 0{\cdot}201\,(8) \times 10^{-4}$ for both models *A* and *B*. The resulting positional and thermal parameters (model *A*) agree within 2σ with those of the conventional X-ray refinement (Teng, Fuess & Bats, 1984).

$MgS_2O_3.6H_2O$

A multipole refinement of the X-ray data of $MgS_2O_3.6H_2O$ was performed in a similar way as for $Na_2S_2O_3$. The atomic coordinate systems are again as in Fig. 1. Although the S_2O_3 group was treated as for $Na_2S_2O_3$, the O atoms of the three water molecules were treated independently, due to differences in their coordination. To avoid excessive numbers of parameters, each water molecule was assigned symmetry $mm2$. The H-atom deformations were constrained to be equal.

At this point it should be realized that the X-ray diffraction experiment for $MgS_2O_3.6H_2O$ only included reflections up to $\sin\theta/\lambda = 0{\cdot}85$ Å^{-1}, whereas for $Na_2S_2O_3$ data were collected up to $\sin\theta/\lambda = 1{\cdot}06$ Å^{-1}. It is well known that the deformation density of O atoms contributes to reflections beyond $\sin\theta/\lambda = 0{\cdot}85$ Å^{-1}. Thus it can be expected that refinement of the deformation density parameters simultaneously with the positional and thermal parameters will result in serious correlations and thus in an ambiguous deformation density (Hermansson, Thomas & Olovsson, 1984). For S this will be less serious, owing to a smaller valence-to-core ratio and the more diffuse nature of the S valence shell. Thus it was decided to refine the multipole parameters together with the S and Mg positional and thermal parameters and the scale and extinction factor. The positional and thermal parameters of O and H, on the other hand, were constrained to the values of the neutron diffraction determination, while for the thermal parameters the correction factors ΔU_{ii} described by Elerman, Bats & Fuess (1983) were added to allow for systematic discrepancies between the two experiments. Convergence was obtained at $wR = 0{\cdot}020$ *versus* $wR = 0{\cdot}026$ for the spherical-atom refinement. At this stage 80 rather weak reflections with $F_{obs}/F_{calc} > 2$ were considered to be affected by multiple reflections and excluded from the data set. Refinement on the remaining 2295 reflections gave $R = 0{\cdot}024$, $wR = 0{\cdot}019$, $S = 1{\cdot}34$; extinction coefficient $g = 0{\cdot}73\,(3) \times 10^{-4}$.

The deformation density

From the deformation density parameters in the two compounds the deformation electron density can be reconstructed in two ways: (i) by using the analytical expressions of the atomic deformation functions; a static deformation density is obtained at infinite resolution; (ii) by a Fourier transform of calculated structure factors; either a dynamic or static electron density is constructed restricted to limited resolution.

It appears doubtful whether an expansion of the electron density beyond the experimental resolution will produce an unambiguous result. Moreover, the second approach is favored for practical reasons, as standard Fourier programs can be applied. Thus we followed that method.

The static deformation densities containing the S–S–O and O–S–O sections of the thiosulfates were calculated for $Na_2S_2O_3$ (both models *A* and *B*) and $MgS_2O_3.6H_2O$. For the first compound reflections up to $\sin\theta/\lambda = 1{\cdot}0$ Å^{-1} were used; for the second

compound the limit was 0·9 Å^{-1}. As only calculated structure factors are needed, all unique data were used including those reflections which were unobserved or suspect in the X-ray diffraction experiment. The result is given in Fig. 2.

The deformation density in both compounds is very similar, notwithstanding large differences in multipole parameters. Thus an interpretation of the individual multipole parameters seems not very meaningful, but instead the deformation density should be considered.

The deformation density in $Na_2S_2O_3$ resulting from model *A*(refinement of all positional parameters) and model *B* (fixing the O positional parameters to values of the neutron diffraction study) is identical near the S atoms. Small differences, however, are observed at the O atoms. Features are more pronounced in model *B*; in particular, the deep trough in the O–S bond at a distance of 0·27 Å from O is not well reproduced in model *A*. The O lone-pair density, though qualitatively similar, is about 0·06 to 0·10 e Å^{-3} lower in model *A* than in *B*. Obviously an experimental resolution of $\sin\theta/\lambda = 1{\cdot}06$ Å^{-1} is not quite sufficient to separate deformation and structural parameters for atoms with steep features in the deformation density such as for O. Bonding features about S have maxima at distances of about 0.7 Å from the S atom and are expected to be well reproduced from X-ray data alone.

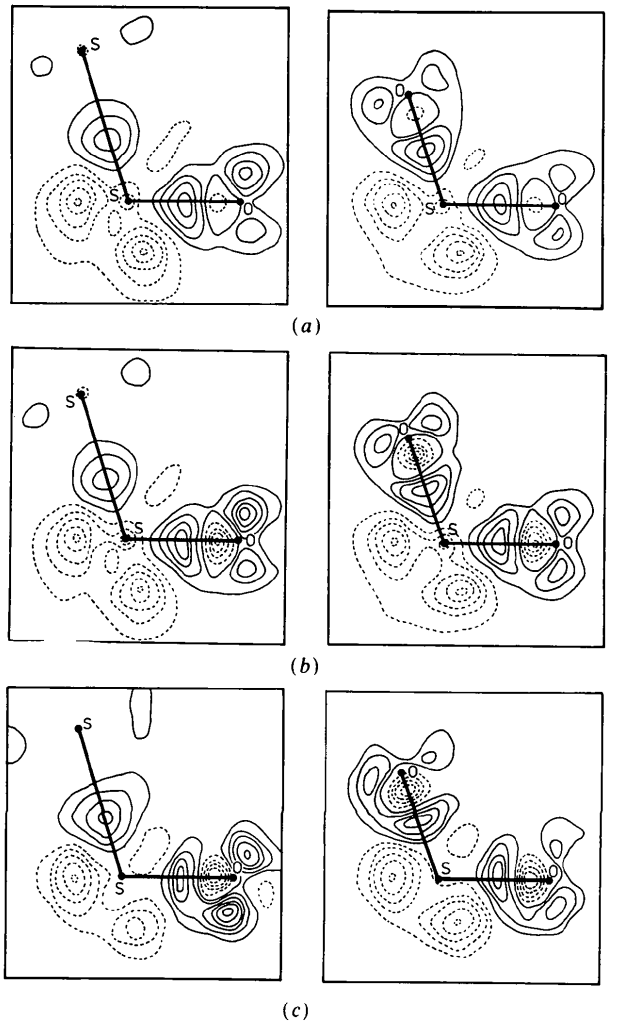

Fig. 2. Static deformation density in the S–S–O and O–S–O sections of the thiosulfate group. Contour interval 0·1 e Å^{-3}, zero contour omitted. (*a*) $Na_2S_2O_3$, multipole refinement model *A*. (*b*) $Na_2S_2O_3$, multipole refinement model *B*. (*c*) $MgS_2O_3.6H_2O$.

The deformation density in the thiosulfate groups in $Na_2S_2O_3$ and $MgS_3O_3.6H_2O$ appears very similar. Peaks of 0·47 e Å^{-3} are found at the midpoints of the S–O bonds in both compounds. Peaks at the midpoints of the S–S bonds are 0·35 and 0·40 e Å^{-3}, respectively. The central S atoms show a considerable charge transfer from the regions at the back of the atoms into the bonds. This has also been observed in charge density studies of other sulfates (Kirfel & Will, 1980, 1981). The thio S atom is characterized by a diffuse ring of density of about 0·12 e Å^{-3} about the S–S axis. It forms an angle of about 90° with the S(1)–S(2) bond. Thus the thio S atom appears to be only slightly hybridized. Although the peak maximum is low, this ring is expected to contain a considerable negative charge due to its large volume. The O lone-pair electrons are found under an angle of about 100° with the O–S bond. Thus the O atoms have a small amount of sp^3 hybridization. A higher density at O is found in the S–S–O than in the O–S–O section. The significance of this effect is not understood.

Characteristic for all O atoms is the deep trough of −0·4 to −0·5 e Å^{-3} close to the O atom in the O–S bond, which is very pronounced in the static deformation density and is reduced to −0·2 e Å^{-3} in the thermally smeared dynamic density. A similar feature is also observed in the *X–N* deformation density of sulfamic acid (Bats, Coppens & Koetzle, 1977) and a theoretical calculation on sulfamic acid (Eisenstein & Cruickshank, 1985) and thus appears no artefact.

The deformation density in the three independent water molecules in $MgS_2O_3.6H_2O$ is shown in Fig. 3. As the static deformation density is free of noise the present result is more suitable to the study of the influence of the intermolecular interactions on the hydrate molecules than the original *X–N* density (Elerman, Bats & Fuess, 1983). The bond peak in the OH bonds amounts to 0·60 e Å^{-3} and is polarized toward H. The H atoms are strongly polarized with an electron-deficient region pointing toward the lone-pair density of the hydrogen-bond acceptor. The shape of the O lone-pair peaks is clearly affected by the coordination type. O(3), which is involved in an O–Mg and O···H–O bond, has a lone-pair region with two separated maxima corresponding to an sp^3-hybridized atom. O(4) and O(5) are both involved in only one Mg–O bond, which lies not far out of the

H-O-H plane, giving these water molecules an approximately trigonal environment. The lone-pair region of these atoms is half-moon shaped with only a single very broad maximum. Thus it appears that the O lone-pair lobe of a tetrahedral hydrate molecule shows two distinct peaks, while a trigonal hydrate molecule shows only one broad peak. A theoretical study of the cation influence on hydrate molecules by Hermansson & Olovsson (1984) shows a depletion of electron density at the O lone-pair lobe near the atomic position in the O–metal direction, which may, however, be obscured in an experimental study. An increase in electron density in the same direction, however, is observed at a distance of about 0·36 Å from O, in agreement with the effect observed in this study.

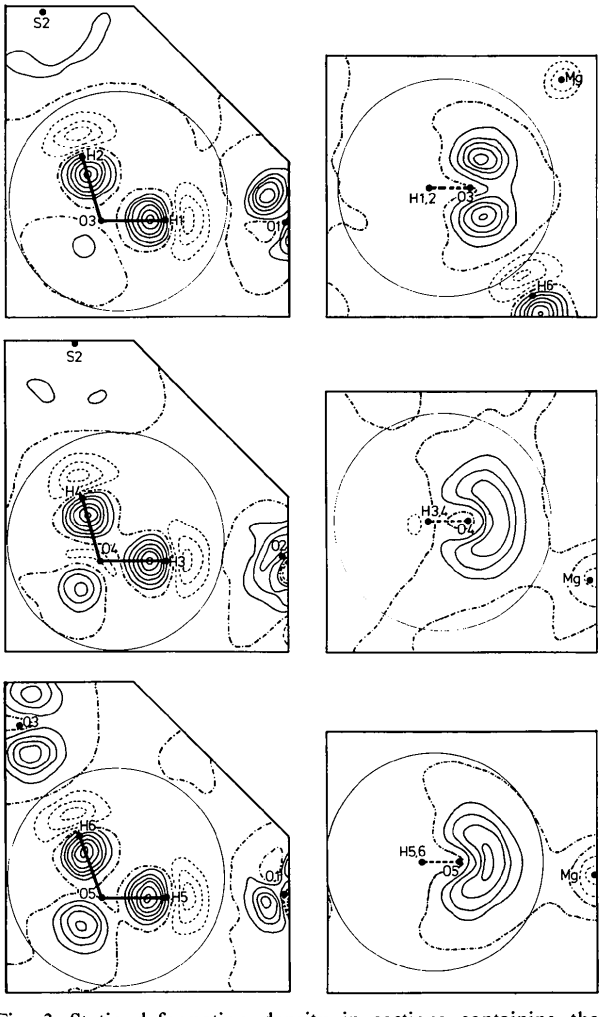

Fig. 3. Static deformation density in sections containing the hydrate group in $MgS_2O_3.6H_2O$. Contour interval 0·1 e Å^{-3}, negative contours dashed, zero contour broken. At left: the plane defined by the HOH group; at right: the plane bisecting the OH bonds. The circles represent spheres with radii of 1·6 Å about the geometrical centers of the water molecules used in the discrete-boundary integration.

Population analysis

In the previous section the deformation density was interpreted in the customary way by contour mapping, allowing for a qualitative interpretation of the electron density in terms of bonding effects. The question arises whether a quantitative derivation of molecular or atomic properties from the observed electron density distribution gives useful results. A molecular or atomic quantity P can be derived by

$$P = \int p(\mathbf{r})\, \delta\rho(\mathbf{r})\, \mathrm{d}v,$$

where $p(\mathbf{r})$ is a function of position and $\delta\rho(\mathbf{r})$ the observed deformation density. For $p(\mathbf{r}) = 1$ the net atomic charge will result; the dipole moment is obtained by $p(\mathbf{r}) = \mathbf{r}$. The integration is either over an atomic volume or over a molecular group of atoms. The usefulness of the result depends on the ability to partition the real space in atomic or molecular volumes. Coppens (1975) defined molecular volumes by the use of effective radii assigned to the atoms. This method is only useful, however, if the valence shells between the molecules do not overlap; that is, for molecular crystals. A more generally applicable way to define atomic volumes has been proposed by Hirshfeld (1977). In this so-called fuzzy-boundary or stockholder method, real space is partitioned in overlapping atomic volumes by the use of atomic weighting functions $w_i(\mathbf{r}) = \rho(\mathbf{r})_{\text{atom } i} / \sum_j \rho(\mathbf{r})_{\text{atom } j}$ where $\rho(\mathbf{r})_{\text{atom } j}$ is the electron density distribution of the neutral, spherical atom j. This method has been used to estimate net charges for the atoms in $Na_2S_2O_3$ and $MgS_2O_3.6H_2O$. The dynamic multipole valence density and sets of atomic valence densities for the chemically different atoms were generated by Fourier summation up to $\sin\theta/\lambda = 1{\cdot}0$ Å^{-1} and using a fine grid division. The net atomic charges were obtained by numerical integration and are reported in Table 2 (3rd column). Variations in $\sin\theta/\lambda$ cut-off showed the net charges to be determined mainly by reflections at small diffraction angles. Series termination appears negligible at $\sin\theta/\lambda = 1{\cdot}0$ Å^{-1}.

For comparison net charges derived from two other methods have been included in Table 2. The first column lists the net charges directly taken from the multipole refinement, while the second column lists those charges resulting from the κ-modified valence-shell projection method *RADIEL* of Coppens, Guru Row, Leung, Stevens, Becker & Young (1979). Net charges from the latter two methods are considerably larger than those of the fuzzy-boundary integration. This may be due in part to contractions or expansions of the atomic valence shells in the latter methods,which considerably change the size of the atomic valence shells so that the resulting charges become rather ambiguous. This problem will not occur for the fuzzy-boundary method, where the atomic volumes are uniquely defined. In formamide

Table 2. *Net atomic charges* (e)

	Multipole refinement	κ refinement	Fuzzy boundary	Fuzzy boundary (ionic model)
$Na_2S_2O_3$				
Na	+0·77 (5)	+0·94 (8)	+0·23	+1·0
S(1)	−0·46(6)	−0·72 (7)	−0·24	−0·78
S(2)	−0·21 (12)	+0·78 (9)	+0·40	+0·17
O	−0·29 (3)	−0·64 (3)	−0·21	−0·45
S_2O_3	−1·54	−1·88	−0.46	−2·0
$MgS_2O_3.6H_2O$				
Mg	+0·81 (20)	+0·12 (23)	+0·32	+2·0
S(1)	−0·68 (7)	−0·92 (8)	−0·39	−0·39
S(2)	−0·17 (9)	+0·36 (14)	+0·19	+0·18
O(*s*)	−0·35 (2)	−0·55 (4)	−0·24	−0·24
O(*w*)	−0·67 (4)	−0·62 (5)	−0·19	−0·42
H(*w*)	+0·42 (3)	+0·48 (2)	+0·15	+0·12
S_2O_3	−1·88	−2·22	−0·93	−0·95
H_2O	+0·18	+0·35	+0·10	−0·18
$Mg(H_2O)_6$	+1·89	+2·21	+0·93	+0·95

considerably smaller net charges were obtained by fuzzy-boundary partitioning in comparison with a κ refinement (Moss, 1982), in agreement with the present result.

Surprising are the rather small positive charges on the alkaline cations: +0·23 e on Na and +0·32 e on Mg in the fuzzy-boundary method. More positive charges are found in the multipole and κ refinements, but were found to be very sensitive to the κ values. Obviously the charges on the alkaline cations are not well defined. The nature of this problem becomes clearer if one considers the radial distribution of the Na and Mg 3*s* valence shells. These are very diffuse and overlap considerably with the surrounding S and O atoms. Figs. 4 and 5 show the effect of integrating the electron density over spheres with radii 0·6, 1·0, 1·5, and 2·0 Å about the metal atoms. The majority of Na and Mg 3*s* electrons are found closer to the S and O atoms than to the metal. In the case of Mg, about 0·6 e lies outside a sphere with radius equal to the Mg–O distance. Integration over the deformation density subtracting Na^+, S^0, and O^0 for $Na_2S_2O_3$ and Mg^{2+}, S^0, O^0, H^0 for $MgS_2O_3.6H_2O$ should give zero charge if the cation really has the ionic charge. As seen from Figs. 4 and 5, this is valid for radii up to 1·0 Å, being the ionic radii of Na^+ and Mg^{2+}. For larger radii the density about the metals rapidly increases and exceeds those of fully occupied 3*s* orbitals already at 1·5 Å. If the integration is performed over the valence density instead of over the deformation density, a very rapid increase in electron density is observed for radii of little more than 1 Å about the metal by penetration into the S and O valence shells. Thus the ionic nature of the metal atoms appears ambiguous. As the fuzzy-boundary partitioning uses the occupied 3*s* shells to assign the volumes of the metals, charge density at the O and S atoms is to some extent assigned to the metals and the small net charges can be understood as artefacts.

If one assumes the alkaline atoms to be ionic, net charges can again be calculated by fuzzy-boundary integration by setting the weighting function of the alkaline atoms to zero. Results thus obtained are given in the fourth column of Table 2. From a comparison of the 3rd and 4th columns, it is seen that in $Na_2S_2O_3$ the Na valence shell shows about twice as much overlap with S(1) as with the remaining atoms. In $MgS_2O_3.6H_2O$ the Mg valence shell overlaps only with the water O atoms but not with the thiosulfate group.

As the ambiguity of the charge on the Mg atom is confined, one would expect the $Mg(H_2O)_6$ cluster as a whole to have a better defined net charge. This value is +0·9 e for the fuzzy-boundary integration but increases to +1·9 e for *MOLLY* and +2·2 e for the κ refinement. Although a considerable charge transfer from cation to anion is observed, the result is not unambiguous. In the present case, about 1 e is not uniquely assigned. As the binding between the $Mg(H_2O)_6$ and S_2O_3 groups consists of O–H···O and O–H···S hydrogen bonds, charge transfer within these hydrogen bonds would be responsible for the different results. The larger charge transfer in *MOLLY* and the κ refinement is understandable from the contraction of the H valence shell and the expansion of the O and S valence shells, which is not accounted for in the fuzzy-boundary method. This effect can be simulated, however, in the fuzzy-boundary integration by using κ-modified atomic valence functions instead of free-atom valence shells. Table 3 gives again the charge distributions in $MgS_2O_3.6H_2O$ by

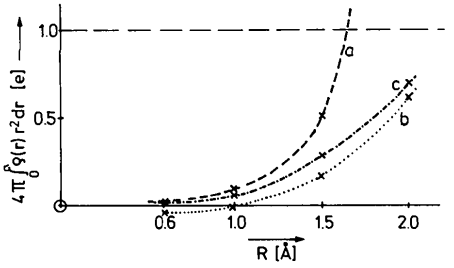

Fig. 4. Integration of the electron density in $Na_2S_2O_3$ over a sphere with radius *R* about the Na atom. (*a*) Experimental valence density. (*b*) Experimental deformation density subtracting Na^+, S^0, O^0 spherical atoms. (*c*) The free-atom Na 3*s* shell.

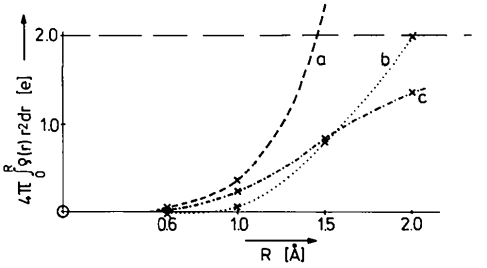

Fig. 5. Integration of the electron density in $MgS_2O_3.6H_2O$ over a sphere with radius *R* about the Mg atom. (*a*) Experimental valence density. (*b*) Experimental deformation density subtracting Mg^{2+}, S^0, O^0, H^0 spherical atoms. (*c*) The free-atom Mg 3*s* shell.

Table 3. *Net atomic charges* (e) *in* $MgS_2O_3.6H_2O$ *by fuzzy-boundary integration using* κ*-modified atomic valence shells*

κ[S(1)]	1·0	1·0	1·0	0·97
κ[O(*s*)]	1·0	1·0	1·0	0·975
κ[O(*w*)]	1·0	1·0	0·975	0·975
κ(H)	1·0	1·40	1·40	1·40
Mg	+0·32	+0·21	+0·26	+0·27
S(1)	−0·39	−0·61	−0·61	−0·65
S(2)	+0·19	+0·10	+0·10	+0·21
O(*s*)	−0·24	−0·32	−0·32	−0·36
O(*w*)	−0·19	−0·23	−0·27	−0·26
H	+0·15	+0·22	+0·23	+0·24
S_2O_3	−0·93	−1·46	−1·46	−1·51
H_2O	+0·10	+0·21	+0·20	+0·21
$Mg(H_2O)_6$	+0·93	+1·46	+1·46	+1·50

fuzzy-boundary integration. In this case also the expansion of the O and S valence shells and the contraction of the H atom on bond formation are considered. In the first column free-atom valence shells have been used to calculate the atomic weighting functions. In the other columns the following κ values were used: $\kappa(H) = 1{\cdot}40$, $\kappa(S) = 0{\cdot}97$ and $\kappa(O) = 0{\cdot}975$. These values were taken directly from the κ refinement. A considerable increase in charge transfer inside the hydrogen bonds is observed when the contracted H atoms are used instead of the free atoms. The use of modified O and S valence shells, however, appears of minor importance. By using the contracted H atoms the charge transfer between $Mg(H_2O)_6$ and S_2O_3 has increased to 1·5 e and approaches the value found in the multipole refinement.

Dipole moment

In contrast to atomic charges which are not observable quantities, the molecular dipole moment can be measured. As a further test as to which of the above methods gives the best charges, the dipole moment average dihedral angle $\bar{\theta}$ are zero to first order in the displacements, and generally finite in higher orders. of the water molecules in $MgS_2O_3.6H_2O$ can be calculated with each of them and compared with the value expected for a free H_2O molecule: $\mu = 1{\cdot}85$ D. It may be noticed that the water molecules in crystalline hydrates are not neutral, so that the observed result depends on the choice of the origin definition. But as long as the net charge on the hydrate is small (+0·1 to +0·2 e), errors are expected to be small when the origin is taken within the molecule. In the present case the geometrical center of the molecule has been used as origin (a point at distance 0·39 Å from O bisecting the H–O–H angle). As the net charges of the bound water molecules are positive, somewhat larger dipole moments are found if the origin is shifted towards O, *i.e.* by the use of the center of mass (being 0·066 Å from O).

The results are reported in Table 4. The fuzzy-boundary integration using $\kappa(H) = 1{\cdot}0$ gives an

Table 4. *Dipole moments* (D) *of the water molecules in* $MgS_2O_3.6H_2O$

	H_2O(I)	H_2O(II)	H_2O(III)
Multipole refinement	2·47 (15)	2·29 (15)	2·48 (15)
κ refinement	2·29 (15)	2·27 (15)	2·10 (15)
Fuzzy boundary $\kappa(H) = 1{\cdot}0$	1·18	1·10	1·48
Fuzzy boundary $\kappa(H) = 1{\cdot}4$	1·69	1·64	1·96
Integration over sphere with radius 1·6 Å	1·57	1·37	2·00

average dipole moment of 1·25 D, which is obviously too small. The fuzzy-boundary method also gives too small a dipole moment for pyridinium-1-dicyanomethylide (Baert, Coppens, Stevens & Devos, 1982). Hirshfeld & Hope (1980) ascribe this effect to a mutual cancellation of overlapping positive and negative densities from expansion functions centered on neighboring molecules. The values of both the multipole refinement (2·4 D) and the κ refinement (2·2 D) seem to overestimate the values expected unless the molecular dipole moment increases on hydration. The fuzzy-boundary integration using $\kappa(H) = 1{\cdot}40$, on the other hand, gives $\mu = 1{\cdot}76$ D in close agreement with the free-molecule value.

Besides the fuzzy-boundary integration, a discrete-boundary integration can also be used to estimate the dipole moment. In the particular case of the hydrate groups, it is noticed that these have a tetrahedral or trigonal environment. Thus the volume occupied by the H_2O molecule is considered to be a sphere. Inspection of the static deformation density of the H_2O molecule in Fig. 3 shows that a sphere of radius 1·6–1·65 Å about the geometrical center of the molecule approximately follows the zero contour line and thus would give an ideal description of the molecular volume. Values obtained in this way using a sphere with radius 1·6 Å are included in Table 4. The results are very similar to those for the fuzzy-boundary integration if $\kappa(H) = 1{\cdot}40$ is used. Thus the dipoles for the hydrate molecules range from 1·6 to 2·4 D depending on the partitioning model used. These values are of the same order of magnitude as the values of 1·92 (5) D (by discrete-boundary integration) and 2·1 (2) D (from multipole refinement) for the water molecule in α-oxalic acid dihydrate (Stevens & Coppens, 1980).

Dipole moments obtained by integration techniques are generally smaller than those obtained by κ or multipole refinement and results from a tail-cutting effect in the former cases (Hirshfeld & Hope, 1980). Errors in the dipole moments derived by integration techniques are not easily obtained from the least-squares covariance matrix and also depend on the volume of integration. Therefore the reliability of the results obtained is best estimated from the spread of values obtained with different methods.

The results of this study can be summarized as follows:

- multipole refinements of accurate X-ray diffrac-

tion data collected at low temperature can provide quantitative descriptions of the deformation density in crystals.

- the deformation density at the O atoms shows steep features which cannot be obtained from X-ray diffraction data up to sin $\theta/\lambda = 1{\cdot}06$ Å^{-1}. In this case atomic parameters of a neutron diffraction study are required.

- spatial partitioning of the electron density using the fuzzy-boundary integration is inadequate for alkaline atoms; for H atoms useful results are obtained, provided contracted atomic basis functions ($\kappa_H = 1{\cdot}4$) are used.

- dipole moments for hydrate molecules range from 1·6 to 2·4 D, depending on the partitioning model used. Thus the method is too crude to estimate changes in the dipole moment on crystal formation.

References

BAERT, F., COPPENS, P., STEVENS, E. D. & DEVOS, L. (1982). *Acta Cryst.* A**38**, 143-151.

BATS, J. W., COPPENS, P. & KOETZLE, T. F. (1977). *Acta Cryst.* B**33**, 37-45.

BECKER, P. J. & COPPENS, P. (1974). *Acta Cryst.* A**30**, 129-147.

COPPENS, P. (1975). *Phys. Rev. Lett.* **34**, 98-100.

COPPENS, P., GURU ROW, T. N., LEUNG, P., STEVENS, E. D., BECKER, P. & YOUNG, Y. W. (1979). *Acta Cryst.* A**35**, 63-72.

EISENSTEIN, M. & CRUICKSHANK, D. W. J. (1985). To be published.

ELERMAN, Y., BATS, J. W. & FUESS, H. (1983). *Acta Cryst.* C**39**, 515-518.

FUKAMACHI, T. (1971). Tech. Rep. Ser. *B*, No. 12. Institute for Solid State Physics, Univ. of Tokyo, Japan.

HANSEN, N. K. & COPPENS, P. (1978). *Acta Cryst.* A**34**, 909-921.

HERMANSSON, K. & OLOVSSON, I. (1984). *Theor. Chim. Acta*, **64**, 265-276.

HERMANSSON, K., THOMAS, J. O. & OLOVSSON, I. (1984). *Acta Cryst.* C**40**, 335-340.

HIRSHFELD, F. L. (1977). *Isr. J. Chem.* **16**, 198-201.

HIRSHFELD, F. L. & HOPE, H. (1980). *Acta Cryst.* B**36**, 406-415.

KIRFEL, A. & WILL, G. (1980). *Acta Cryst.* B**36**, 512-523.

KIRFEL, A. & WILL, G. (1981). *Acta Cryst.* B**37**, 525-532.

MOSS, G. (1982). *Electron Distribution and the Chemical Bond*, edited by P. COPPENS & M. B. HALL, pp. 383-411. New York: Plenum.

STEVENS, E. D. & COPPENS, P. (1980). *Acta Cryst.* B**36**, 1864-1876.

TENG, S. T., FUESS, H. & BATS, J. W. (1981). *Z. Kristallogr.* **154**, 337-338.

TENG, S. T., FUESS, H. & BATS, J. W. (1984). *Acta Cryst.* C**40**, 1785-1787.

Acta Cryst. (1986). B**42**, 32-39

Structures of the Basic Zinc Sulfates $3Zn(OH)_2.ZnSO_4.mH_2O$, $m = 3$ and 5

BY I. J. BEAR, I. E. GREY,* I. C. MADSEN, I.E. NEWNHAM AND L. J. ROGERS

CSIRO Division of Mineral Chemistry, PO Box 124, *Port Melbourne, Victoria* 3207, *Australia*

(*Received* 5 *April* 1985; *accepted* 16 *August* 1985)

Abstract

The basic zinc sulfate $3Zn(OH)_2.ZnSO_4.5H_2O$ has triclinic symmetry, $P\bar{1}$, $a = 8{\cdot}354(2)$, $b = 8{\cdot}350(2)$, $c = 11{\cdot}001(2)$ Å, $\alpha = 94{\cdot}41(2)$, $\beta = 82{\cdot}95(2)$, $\gamma = 119{\cdot}93(2)°$, $Z = 2$, $M_r = 549{\cdot}54$, $V = 659{\cdot}9(3)$ Å^3, $D_x = 2{\cdot}77$ g cm^{-3}, λ(Mo $K\bar{\alpha}$) = 0·71069 Å, $\mu = 75{\cdot}54$ cm^{-1}, $F(000) = 544$. Dehydration at room temperature in the water-vapour-pressure range pH_2O = 1-5 mm (~10-50 Pa) gives the trihydrate, $3Zn(OH)_2.ZnSO_4.3H_2O$, symmetry $I\bar{1}$, $a = 8{\cdot}367(3)$, $b = 8{\cdot}393(3)$, $c = 18{\cdot}569(5)$ Å, $\alpha = 90{\cdot}29(3)$, $\beta = 89{\cdot}71(3)$, $\gamma = 120{\cdot}53(3)°$, $Z = 4$, $M_r = 513{\cdot}54$, $V = 1123{\cdot}2(6)$ Å^3, $D_x = 3{\cdot}04$ g cm^{-3}, $\mu = 88{\cdot}52$ cm^{-1}, $F(000) = 1008$. The structures were refined to final wR values of 0·031 and 0·13 for the pentahydrate and the trihydrate respectively, using 2319 and 1120 independent reflections with $I > 3\sigma(I)$. The structures of both compounds comprise modified $Zn(OH)_2$ layers, alternating with layers of water molecules along **c**. The modified $Zn(OH)_2$ layers are CdI_2-type sheets of edge-shared octahedra, with one-seventh of the octahedral sites vacant and with composition $[Zn_6\square(OH)_{12}O_2]^{4-}$. Tetrahedrally coordinated Zn atoms, $[Zn(OH)_3H_2O]^{1-}$, are located above and below the empty sites and corner-share their basal hydroxides with six octahedra. Sulfate groups connect on either side of the octahedral sheets by corner sharing. The composition of the complete neutral layer is $[Zn_6^{VI}\square(OH)_6.Zn_2^{IV}(OH)_6(H_2O)_2.(SO_4)_2]$. The layers are held together by strong hydrogen bonding between the coordinated and free water molecules and the basal O atoms of the sulfate groups. A dehydration mechanism is proposed.

1. Introduction

Basic zinc sulfates have been studied for more than 150 years (Kuhn, 1830) and during this time a vast literature has accumulated on the characterization of a wide range of salts with the general formula $nZn(OH)_2.ZnSO_4.mH_2O$, $1 \le n \le 7$ and $0 \le m \le 5$,

* Author to whom correspondence should be addressed.

0108-7681/86/010032-08$01.50 © 1986 International Union of Crystallography